Received: 25 August 2016 | Accepted: 7 November 2016
DOI 10.1002/hyp.11077

WILEY

RESEARCH ARTICLE

Stable isotope variations of precipitation and streamflow reveal the young water fraction of a permafrost watershed

Chunlin Song[1,2] | Genxu Wang[1] | Guangsheng Liu[3] | Tianxu Mao[1] | Xiangyang Sun[1] | Xiaopeng Chen[1,2]

[1] Institute of Mountain Hazards and Environment, Chinese Academy of Sciences, Chengdu 610041, China
[2] University of Chinese Academy of Sciences, Beijing 100049, China
[3] College of Environmental Science and Engineering, Xiamen University of Technology, Xiamen 361024, China

Correspondence
Genxu Wang, Institute of Mountain Hazards and Environment, Chinese Academy of Sciences, Chengdu 610041, China.
Email: wanggx@imde.ac.cn

Funding information
National Natural Science Foundation of China, Grant/Award Number: 91547203, 41401044; National Basic Research Program of China, Grant/Award Number: 2013CBA01807.

Abstract
The streamflow age is an essential descriptor of catchment functioning that controls runoff generation, biogeochemical cycling, and contaminant transport. The young water fraction (F_{yw}) of streamflow, which can be accurately estimated with tracer data, is effective at characterizing the water age proportions of heterogeneous catchments. However, the F_{yw} values of permafrost catchments are not known. We selected a watershed in the permafrost region of the Qinghai-Tibet Plateau (QTP) as our study area. Daily interval stable isotopes (deuterium and oxygen-18) of precipitation and streamflow were studied during the 2009 thawing season. The results show that the stable isotope compositions of precipitation and stream water have significant spatial and temporal variations. HYSPLIT backwards trajectory results demonstrate that the moisture in the study area mainly derived from the westerlies and southern monsoons. Thawing processes in the active layer of the permafrost significantly altered the stable isotope compositions of the stream water. The soil temperature, soil moisture, and air temperature are the main drivers of the stable isotope variations in the stream water. We estimated the young water fractions of the five catchments in the study area, which were the first estimates of the F_{yw} in permafrost catchments in the QTP. The results show that an average of 15% of the streamflow is younger than 43 days. Additional analyses show that the vegetation cover significantly controls the young water fraction of the streamflow. These results will improve our understanding of permafrost hydrological processes and water resource utilization and protection.

KEYWORDS
permafrost hydrology, Qinghai-Tibet Plateau, stable isotopes, watershed hydrology, young water fraction

1 | INTRODUCTION

Stable isotopes (deuterium and oxygen-18) are recognizable tracers that are related to the water cycle and have been widely used in hydrology and water resources for decades (Gat, 1996). As effective tracers, stable isotopes have been applied for hydrography separation, water source identification, mean transit time (MTT) estimations, and hydrological process quantification at a variety of spatial and temporal scales (Pearce, Stewart, & Sklash, 1986; Hinton, Schiff, & English, 1994; Jonathan A Foley, 1996; Klaus & McDonnell, 2013; Tekleab, Wenninger, & Uhlenbrook, 2014; Jasechko, Kirchner, Welker, & McDonnell, 2016). The spatial and temporal variations of stable hydrogen and oxygen isotopes in precipitation are affected by the moisture sources, elevation, temperature, rainfall amount, latitude, and distance from oceans (Rozanski, Araguas-Araguas, & Gonfiantini, 1992; Gat, 1996; Yao et al., 2013). In permafrost regions, the hydrological processes are mainly affected by the dynamics of the active soil layer (the shallow soil layer above the permafrost that thaws in the summer and freezes in the winter; Zhang, Ohata, & Kadota, 2003; Wang, Hu, & Li, 2009; Wang, Liu, & Liu, 2011; Streletskiy et al., 2015). However, few observational studies have been conducted on the hydrological features and processes in permafrost regions of the Qinghai-Tibet Plateau (QTP) using stable isotope techniques (Cuo, Zhang, Zhu, & Liang, 2014).

Runoff generation, biogeochemical cycling, and contaminant transport are regulated by the age of the streamflow, which is an essential descriptor of catchment functioning and is defined as the time required for precipitation to travel through water channels and reach streams (McGuire & McDonnell, 2006; Maher, 2010; McDonnell et al., 2010). The seasonal cycles of stable isotope tracers in water can be used to characterize the MTT of catchments, which is the average travel time for water parcels to enter as precipitation and leave as streamflow within catchments. Seasonal cycles of stable isotope tracers have been used to estimate the MTT at many sites (Rodgers, Soulsby, & Waldron, 2005; McGuire & McDonnell, 2006; Soulsby, Tetzlaff, Rodgers, Dunn, & Waldron, 2006; Tekleab et al., 2014). However, a recent study showed that most of these calculations have errors of several hundred percent because of aggregation bias (Kirchner, 2016a). Kirchner (2016a) proposed an alternative metric, the young water fraction (F_{yw}), which is defined as the proportion of the transit-time distribution that is younger than a certain threshold age (τ_{yw}). F_{yw} is a better metric than MTT because it can be accurately estimated from the amplitude ratio of seasonal tracer cycles in precipitation and runoff with a precision of a few percent. F_{yw} is reliable for heterogeneous real world catchments and is thus much less uncertain than the MTT. Jasechko et al. (2016) recently calculated the F_{yw} values of hundreds of catchments around the world and found that nearly one-third of the global river water is less than 3 months old. In permafrost regions, the age of groundwater ranges from approximately 1 to 55 years (Hiyama, Asai, Kolesnikov, Gagarin, & Shepelev, 2013). However, the age composition of the streamflow in permafrost regions is still unknown.

The QTP is often called the "Third Pole" or the "Water Tower of Asia" and is the headwater of many large Asian rivers, including the Yangtze, Yellow, and Lancang Rivers. Hydrological changes in the QTP are critical to the safety of freshwater resources in these rivers. Because it is the only mid-latitude permafrost region, the QTP is considered to be more sensitive to climatic warming than higher latitude Arctic regions (Wang & French, 1995; Zhang et al., 2003; Wang et al., 2011). This study uses the Zuomaokong watershed, which is a typical permafrost catchment in the QTP, as the study site. Previous hydrological studies of this site have examined vegetation-hydrological process interactions, thermal soil effects, and the effects of active soil layer freeze–thaw cycles on hydrological processes (Wang, Li, Hu, & Wang, 2008; Wang et al., 2009; Wang et al., 2011; Wang, Liu, Li and Yang, 2012b; Wang, Mao, Chang and Liu, 2015). However, the relationships between freeze–thaw processes and stream water stable isotopes are unclear. No studies have examined such permafrost catchments to characterize streamflow ages using isotopic tracers. The young water fraction of such permafrost watersheds remains unknown. To better understand permafrost hydrological processes, we conducted daily interval sampling of precipitation and streamflow in the Zuomaokong watershed in 2009 and measured the deuterium and oxygen-18 values of the samples. Using the continuous and high-resolution stable isotope series, the main objectives of this study are: (a) to characterize the spatiotemporal variations of the stable isotopes and (b) to estimate the young water fraction of stream water through stable isotope tracers.

2 | SITE DESCRIPTION

This study was conducted in the Zuomaokong watershed, which is a secondary tributary of the Yangtze River that is located in the hinterland of the QTP (Figure 1). The total watershed area covers 127.63 km^2, and the elevation of the watershed ranges from 4,720 to 5,932 m a.s.l. We divided the watershed into five catchments with areas of 10.9 to 112.5 km^2 (Figure 1). Table 1 presents the characteristics of the catchments.

The study area is characterized by a cold and dry continental alpine climate with a mean annual air temperature of −5.2 °C and annual mean precipitation of 328.9 mm. The average summer and winter temperatures are 6.2 °C and −13.2 °C, respectively. The peak temperatures occur in July and August, and the monthly mean air temperature is greater than 0 °C from May to September. Precipitation events that occur from June to September account for 83% of the total annual precipitation, and the highest precipitation occurs in July and August. During the freezing season from November to April, the total precipitation is normally less than 5 mm, and the river channel usually contains no liquid water for sampling. The relative humidity ranges from 17% to 96% in the winter and summer, respectively.

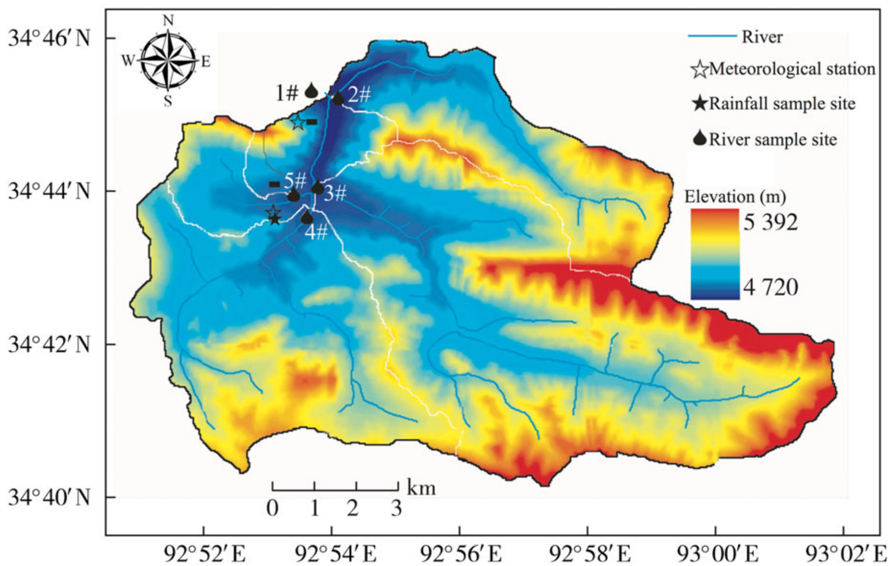

FIGURE 1 Location map showing the Zuomaokong watershed. The stream water and precipitation sampling sites are marked

TABLE 1 Characteristics of the catchments in the study area

Catchment number	Drainage area (km^2)	Mean slope gradient	Mean elevation (m)	Area ≥ 5000 m (%)	Mean runoff coefficient	Swamp meadow (%)	Vegetation coverage (%)
1	112.5	0.042	4922	22.2	0.47	4.4	43.4
2	17.8	0.046	4915	20.2	0.49	3.3	32.3
3	54.5	0.041	4948	32.1	0.34	5.0	37.9
4	29.3	0.040	4905	10.5	0.29	2.5	52.5
5	10.9	0.045	4834	5.7	0.81	10.7	57.3

The Zuomaokong watershed is a typical permafrost region with permafrost depths that vary from 60 to 120 m and an active layer that ranges from 1.3 to 2.5 m (Wang et al., 2011). The study area is characterized by alpine meadow and swamp vegetation, and the main types of vegetation include *Kobresia pygmaea*, *Kobresia humilis* and *Kobresia capilifolia*. Catchment 5 has the highest degree of vegetation coverage (57.3%), whereas catchment 2 has the lowest degree of vegetation coverage (32.3%). The freezing season usually occurs from November to the following May. The annual runoff outside the freezing season includes two flooding periods (Figure 2) and three dry periods, including a summer flooding period that starts in July with a slight recession period in August, an autumn flooding period in September with a baseflow recession from late September to October, and a third dry season from November to the following April.

3 | METHODS

3.1 | Field sampling and measurements

Compared to weekly sampling, a higher sampling frequency (e.g., daily) will provide more information about hydrological processes and improve stream isotope simulations (Stockinger et al., 2016). We conducted daily interval stream water sampling campaigns in the five catchments of the Zuomaokong watershed during the 2009 thawing season (i.e., May to October) because stream water sampling is impossible during the freezing season (i.e., November to April). Precipitation samples were collected after every day of precipitation in catchment 4 within the basin to represent the entire watershed. When more than one precipitation event occurred in a day, the δ value of the isotopes in the precipitation was calculated as the weighted mean composition of the rainfall. Daily stream water samples were collected manually at the outlets of the five sub-catchments (Figure 1). During the sampling period, all of water samples were deposited into 50 ml high-density polyethylene (HDPE) bottles, which were then closed immediately and subjected to cold preservation at 4 °C to prevent fractionation due to evaporation. We collected 72 precipitation samples and 567 stream water samples during the sampling period.

A runoff observation system with gauging instruments was installed along the catchment outlets before we started our investigation. Daily discharge and water level data for the entire catchment were collected. Soil moisture levels were measured using a frequency domain reflectometer (FDR) with a calibrated soil moisture sensor equipped with a Theta probe (Holland Eijkelamp Co.). Soil temperature was monitored using a thermal resistance sensor with a temperature sensitivity range of −40 to +50 °C and a system precision of ±0.02 °C. Soil moisture and temperature were measured every 2 h from April to November and twice daily (between 9 and 11 a.m. and between 15 and 17 p.m.) from December to March. The soil freezing depth was determined based on the measured soil temperature (0 °C is the threshold of soil freezing and thawing). Precipitation and air temperature data were collected at the meteorological station located at the outlet of the Zuomaokong watershed with two portable micro-meteorological stations (Figure 1).

3.2 | Laboratory analysis

The isotope compositions of all of the water samples were analysed at the Key Laboratory of Mountain Surface Processes and Ecological Regulation at the Chinese Academy of Sciences Institute of Mountain Hazards and Environment using an LGR DLT-100 liquid-water isotope analyser (Los Gatos Research, Inc., USA). The stable isotopic compositions of oxygen-18 and deuterium are reported in δ notation (‰, parts per million), which is defined based on the Vienna Standard Mean Ocean Water (VSMOW) measure with δD and $\delta^{18}O$ (where $\delta^{18}O = [(^{18}O/^{16}O_{sample})/(^{18}O/^{16}O_{VSMOW}) - 1] \times 10^3$‰; similar for δD). We use the weighted isotopic composition of the precipitation for

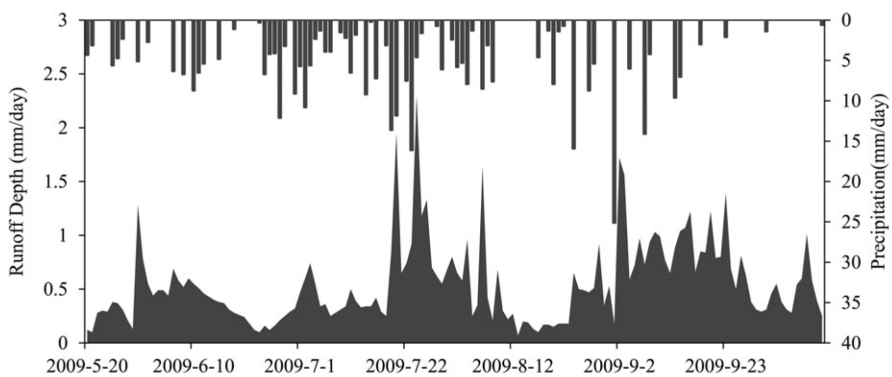

FIGURE 2 Daily precipitation and discharge for the Zuomaokong watershed during the study period

the analysis. The analytical precision of the liquid-water isotope analyser measurements was ±0.2‰ for $\delta^{18}O$ and ±1‰ for δD.

3.3 | HYSPLIT backward trajectory model

Potential moisture sources of daily precipitation in the Zuomaokong watershed were studied using the Hybrid Single Particle Lagrangian Integrated Trajectory (HYSPLIT) model (Draxler, 1998; http://www.arl.noaa.gov/HYSPLIT_info.php), which was developed through the Air Resources Laboratory of the National Oceanic and Atmospheric Administration (NOAA). The HYSPLIT model has been widely used for atmospheric transport (Stein et al., 2015) and moisture source determinations (Tekleab et al., 2014; Sánchez-Murillo et al., 2016). The HYSPLIT model provides complete modeling environments for computing simple air parcel trajectories and complex transport processes using a three-dimensional Lagrangian air mass velocity algorithm. In our study, the air parcel trajectories were modeled for 240 h backwards in time because the study site is far from any ocean. To compute a trajectory, the HYSPLIT model requires a starting time, geographic information (i.e., coordinates and elevation) and NOAA meteorological data files. The entire sampling period was divided into the spring (2009-6-21 to 2009-8-8) and summer (2009-8-17 to 2009-10-12) flooding seasons. Daily backward trajectories for each rain sample from the two flood seasons were computed.

3.4 | Young water fraction calculation

The young water fraction (F_{yw}) is defined as the proportion of water that is younger than a specific threshold age. F_{yw} is a more reliable metric than MTT to characterize the streamflow age composition within a precision of a few percent. Kirchner (2016a) developed the approach to calculate the young water fraction in heterogeneous and nonstationary catchments, and (Jasechko et al., 2016) used the approach to calculate the young water fractions of hundreds of rivers around the globe. We calculated F_{yw} for each catchment following the methodology developed by Kirchner (2016a). First, we performed sine wave regressions on the $\delta^{18}O$ (‰) time series to determine the cosine and sine coefficients of the precipitation and streamflow:

$$\begin{aligned} C_P(t) &= a_P\cos(2\pi ft) + b_P sin(2\pi ft) + k_P, \\ C_S(t) &= a_S\cos(2\pi ft) + b_S sin(2\pi ft) + k_S \end{aligned} \quad (1)$$

where $C_P(t)$ and $C_S(t)$ are the $\delta^{18}O$ (‰) compositions of the precipitation and streamflow, respectively, k_P and k_S are the vertical shifts of the fitted sine waves, f is the frequency of the annual fluctuations (set to 1/365 days; i.e., 1 per year), t is the time in days after the start of the sampling period, and a_p, b_p, a_s, *and* b_s are coefficients for determining the amplitude and phase shift of the seasonal $\delta^{18}O$ cycles:

$$A_P = \sqrt{a_P^2 + b_P^2},\ \ A_S = \sqrt{a_S^2 + b_S^2} \quad (2)$$

$$\varphi_P = tan^{-1}\left(\frac{a_P}{b_P}\right),\ \ \varphi_S = tan^{-1}\left(\frac{a_S}{b_S}\right) \quad (3)$$

where A_p and A_s are the amplitudes of the precipitation and streamflow, respectively, and φ_p and φ_s are the phase shifts of the precipitation and streamflow, respectively.

The difference between the sine shifts of the precipitation and streamflow sine waves $\varphi_s – \varphi_p$ can be expressed as a function of the shape parameter α (Stockinger et al., 2016):

$$\varphi_S – \varphi_P = \alpha tan^{-1}\sqrt{(A_S/A_P)^{-2/\alpha} – 1} \quad (4)$$

By iteratively solving this equation, we use α to calculate the scale parameter β and the threshold age (τ_{yw}) of the young water fraction (Kirchner, 2016a):

$$\beta = \frac{1}{2\pi f}\sqrt{(A_S/A_P)^{-2/\alpha} – 1} \quad (5)$$

$$\tau_{yw} = 0.0949 + 0.1065\alpha – 0.0126\alpha^2\ \left(R^2 = 0.9998\right) \quad (6)$$

The final step is to calculate F_{yw} using the regularized lower incomplete gamma function $\Gamma(\tau_{yw},\alpha,\beta)$:

$$F_{yw} = \Gamma(\tau_{yw}, \alpha, \beta) = \int_{\tau=0}^{\tau_{yw}} \frac{\tau^{\alpha-1}}{\beta^{\alpha}\Gamma(\alpha)} e^{-\frac{\tau}{\beta}} d\tau \quad (7)$$

According to Kirchner (2016a), F_{yw} was solved by numerical experiments and is nearly equivalent to the amplitude ratio A_s/A_p.

After the calculations of F_{yw} and τ_{yw}, we estimated the uncertainty ranges of F_{yw} and τ_{yw} with the method described by Stockinger et al. (2016): by first adding and second subtracting the standard error to the estimates of the coefficients (i.e., a_p, b_p, a_s, *or* b_s) which were less significant, we obtained the ranges of the coefficients. Then, we recalculated the lower and higher ranges of F_{yw} and τ_{yw} for each catchments with the ranges of the coefficients.

3.5 | Statistical analysis

A Pearson's correlation analysis was conducted to identify potential relationships between the isotope values and environmental variables. We then conducted a stepwise regression analysis to determine the key predictive variables of the stable isotopes. We first selected soil moisture and temperature data at different depths as different predictive variables, which over-fit the regression model due to multicollinearity. Thus, we chose the mean values of the soil moisture and temperature at different depths to fit the multiple linear regression models while avoiding multicollinearity and to generate multiple linear regression models that reveal the main drivers of the isotope variations. Finally, we performed sine wave regressions to calculate the young water fractions of the stream water at different spatial scales. The statistical analysis was completed using the R language (R Core Team, 2016), and the significance level of the hypothesis tests was 0.05.

4 | RESULTS AND DISCUSSION

4.1 | Meteoric water lines

During the sampling period, the $\delta^{18}O$ values of the precipitation in the Zuomaokong watershed ranged from −21.0 to 3.1‰ with a mean value of −8.2‰, and the δD values ranged from −189 to 43‰ with a mean value of −58‰. The $\delta^{18}O$ values of the stream water in the Zuomaokong watershed ranged from −13.3 to −4.8‰ with a mean value of −9.1‰, and the δD values ranged from −101 to −27‰ with a mean value of −66‰ (Table 2).

Figure 3a shows the linear relationships of the δD and $\delta^{18}O$ ratios of the precipitation as Local Meteoric Water Lines (LMWLs) in comparison with the Global Meteoric Water Line (GMWL). The δD-$\delta^{18}O$ relationships of the stream water of the sub-catchments are plotted in Figure 3b for comparison. Craig (1961) reported the GMWL based on global samples from rivers, lakes, and precipitation with the relationship of $\delta D = 8\delta^{18}O + 10‰$. The LMWL of precipitation in the Zuomaokong watershed ($\delta D = 9.57\delta^{18}O + 24.01‰$, $n = 72$, $R^2 = 0.96$, $p < 0.001$) has a steeper slope and greater intercept than the GMWL. The high slope of the LMWL (9.57) in the study area reflects the complex moisture sources and local recycling processes on the QTP (Yao et al., 2013). The deviation of the LMWL from the GMWL might reflect the different compositions of convective and stratiform rain in the precipitation (Aggarwal et al., 2016). Similar relationships between the concentrations of stable hydrogen and oxygen isotopes in the meteoric water of the QTP were observed in previous studies (Yu et al., 2007; Yao et al., 2013). However, the difference between the LMWL of the stream water ($\delta D = 5.01\delta^{18}O–20.48‰$, $n = 567$, $R^2 = 0.47$, $p < 0.001$) and the GMWL cannot be neglected. The slope of the LMWL of the stream water (5.01) is lower than that of the GMWL and LMWL of the precipitation. The stream flow of the Zuomaokong watershed is largely controlled by thawing and freezing of the active soil layer (Wang et al., 2009). Soil and surface water evaporation may induce lower slope of water lines due to water loss and more enriched isotopic values (Sugimoto et al., 2003; Sánchez-Murillo et al., 2015). Thus, the water lines of the stream water exhibit relative low slopes (Table 2, 4.15–5.5). Similar results of low slopes of stream water lines were found in the inland watersheds of the Pacific Northwest (Sánchez-Murillo et al., 2015). Furthermore, due to the dry climate and the mean annual precipitation of 328.9 mm in the Zuomaokong watershed, open water evaporation might also be a factor that regulates the relationships of δD and $\delta^{18}O$ in stream water (Craig, 1961; Zhao et al., 2011; Cui and Li, 2015), which is consistent with studies of major Chinese rivers (Li et al., 2014). The evaporation of stream water might potentially increase the uncertainty of the F_{yw} estimation due to its impact on isotopic signals. The intercept of the stream water LMWL is more negative than those of the GMWL and the LMWL of precipitation, which is similar to rivers in cold regions of China (Li et al., 2014). Table 2 also shows the LMWLs of the five sub-catchments in the Zuomaokong watershed; the small differences between the LMWLs are reasonable due to the heterogeneity of the catchments.

TABLE 2 Summary of δD(‰), $\delta^{18}O$(‰), and LMWLs in Zuomaokong watershed

Sample	Site	Average δD (‰)	Average $\delta^{18}O$ (‰)	LMWLs
Precipitation	Zuomaokong watershed	−58	−8.2	$\delta D = 9.57\delta^{18}O + 24.01‰$, $n = 72$, $R^2 = 0.96$, $p < 0.001$
Stream water	Catchment 1	−68	−9.4	$\delta D = 5.46\delta^{18}O–16.76‰$, $n = 114$, $R^2 = 0.47$, $p < 0.001$
	Catchment 2	−66	−9.2	$\delta D = 5.45\delta^{18}O–15.72‰$, $n = 114$, $R^2 = 0.40$, $p < 0.001$
	Catchment 3	−68	−9.2	$\delta D = 5.50\delta^{18}O–17.07‰$, $n = 113$, $R^2 = 0.49$, $p < 0.001$
	Catchment 4	−66	−9.2	$\delta D = 4.15\delta^{18}O–28.26‰$, $n = 114$, $R^2 = 0.33$, $p < 0.001$
	Catchment 5	−63	−8.5	$\delta D = 4.77\delta^{18}O–22.01‰$, $n = 112$, $R^2 = 0.39$, $p < 0.001$
	All stream water	−66	−9.1	$\delta D = 5.01\delta^{18}O–20.48‰$, $n = 567$, $R^2 = 0.47$, $p < 0.001$

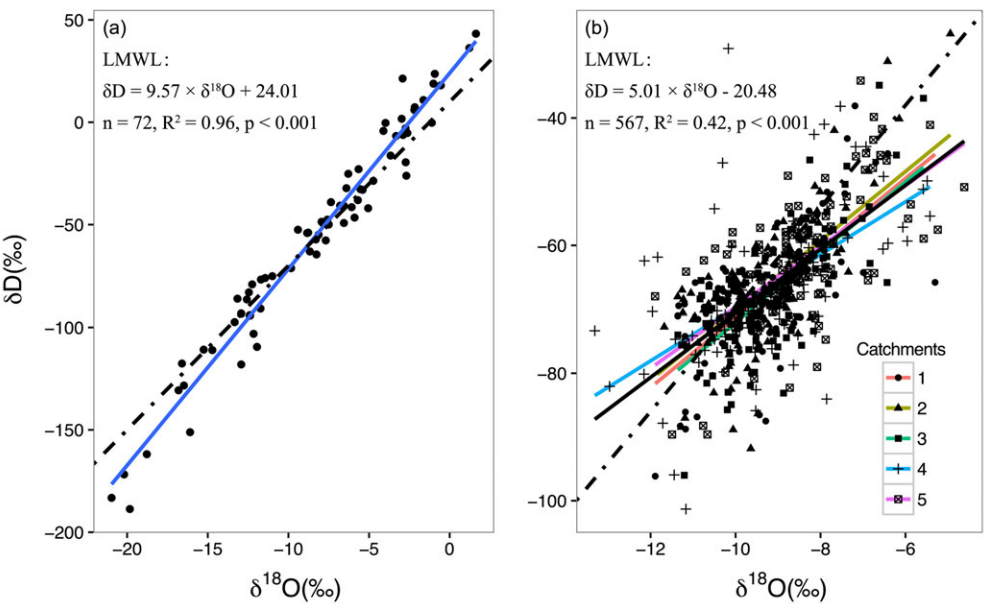

FIGURE 3 Relationships between δD and $\delta^{18}O$ for precipitation (a) and stream water (b) in Zuomaokong watershed. In (a) and (b): Solid line is the Local Meteoric Water Line (LMWL); dot dash line is the Global Meteoric Water Line (GMWL), which expressed as a worldwide average formula of $D = 8 \times \delta^{18}O + 10‰$

4.2 | Spatiotemporal variations of stable isotopes and potential drivers

4.2.1 | Isotope variations of precipitation

Figure 4a shows the time series of the measured $\delta^{18}O$ values for precipitation. The variations of the stable hydrogen and oxygen isotope compositions of the precipitation are greater than those of the stream water. The isotope composition of precipitation increases from late May to early June, decreases from June to mid-July, increases until mid-August, and decreases until October. Previous studies have identified effects from the amount of precipitation (negative correlation between the isotope values and the amount of rainfall), elevation (the isotopic compositions of meteoric water in mountainous regions are more heavily depleted at higher elevations) and temperature (the isotopic compositions of precipitation are positively correlated with temperature) that control the stable isotopic compositions of precipitation (Dansgaard, 1964; Siegenthaler and Oeschger, 1980; Rozanski et al., 1992; Yao et al., 2013; Sánchez-Murillo et al., 2016). Rainfall and temperature effects that show negative and positive correlations of the isotopic composition with the amount of rainfall and temperature variations, have also been found in other regions of the QTP (Yao et al., 2013). As the temperature increased rapidly from May to June, the isotopic composition of the precipitation also increased (Figure 4a). The physical basis of the temperature effects is that equilibrium fractionation is strongly temperature dependent (Gat, 1996). The higher temperatures cause more evaporation and thus higher isotopic values. The increasing isotopic compositions between July and August are accompanied by decreasing precipitation in late July and early August (Figure 4a). As a result, the "precipitation amount effect" that caused the negative correlation between rainfall levels and isotopic composition may have caused the increases in isotope composition (Rozanski et al., 1992; Gao et al., 2009; Sánchez-Murillo et al., 2016). Greater amounts of rainfall reduce the probability of moisture fractionation during the travel of a raindrop towards the ground (Sánchez-Murillo et al., 2016). Thus, more rain will generate less depleted isotope values of the precipitation. On the other hand, changes in storm characteristics might also be responsible for the isotope variations of precipitation (Sánchez-Murillo et al., 2016).

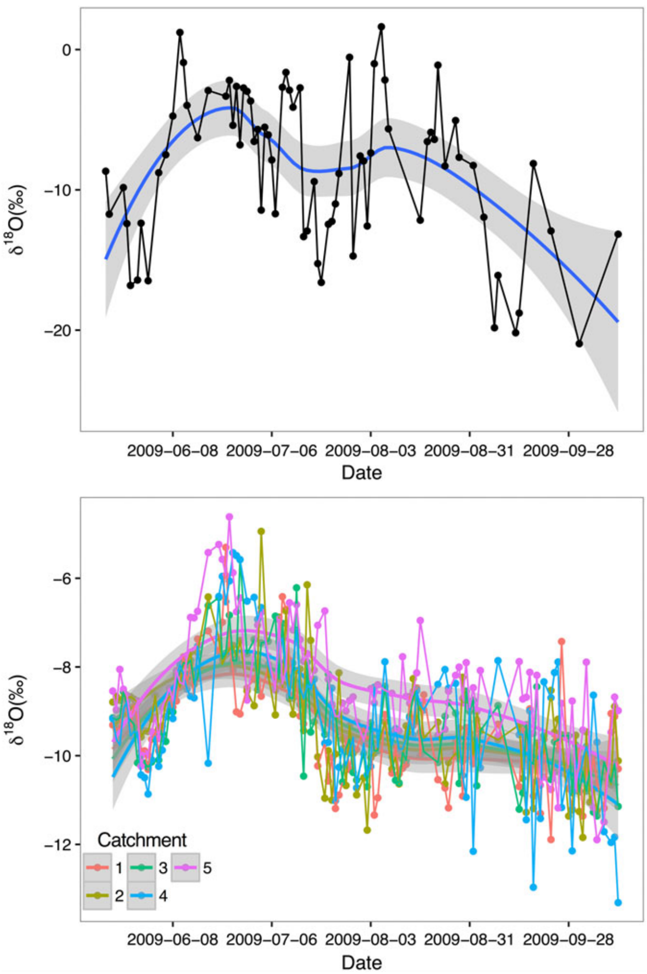

FIGURE 4 Temporal variations of $\delta^{18}O$ values in precipitation (a) and stream water (b). The grey shades are confidence level of 95%

4.2.2 | Implications from the HYSPLIT model

The potential moisture sources of the daily rainfall events that were sampled at the study site were identified using the HYSPLIT backwards trajectory model. The entire sampling period was divided into spring (2009-6-21 to 2009-8-8) and summer (2009-8-17 to 2009-10-12) flooding seasons. Daily backward trajectories for each rain sample from the two flooding seasons were calculated (Figure 5). The moisture sources of the QTP include three domains, the westerlies, the Bay of Bengal (BOB) and southern Indian Ocean, and the East Asian monsoon, and they change with the season (Tian et al., 2001; Yu et al., 2007; Hren et al., 2009; Yao et al., 2013). The moisture transport trajectory results for our study site are consistent with these domains. During the spring flooding season, most of the moisture came from the East Asian and westerly regions combined with interactions between regional air masses. During the summer flooding season, the southern Indian subcontinent and westerly moisture sources contributed the majority of the rainwater. The variations in the time series of the isotope values (Figure 4) also confirm the complexities of the moisture sources and transport processes. The long-range transport of moisture from the oceans showed greater isotopic fractionation with increasing inland distance, which resulted in more depleted isotope values of the meteoric water. This "continental effect" encapsulates several processes, including the levels of evapotranspiration and the advection transport ratio by eddy diffusion (Winnick et al., 2014). In addition, as the world's tallest and largest plateau, the high elevations of the QTP enhances the elevation effects during moisture transport (Yao et al., 2009, 2013). Therefore, the spring flooding season, which has more long-range moisture sources, exhibits more depleted isotope values than the summer flood season.

4.2.3 | Isotope variations of stream water

The isotopic composition of the stream water during the study period is more constant than that of the precipitation (Figure 4b) because stream water is not only affected by precipitation but is also recharged by soil water and groundwater, which have constant isotopic compositions

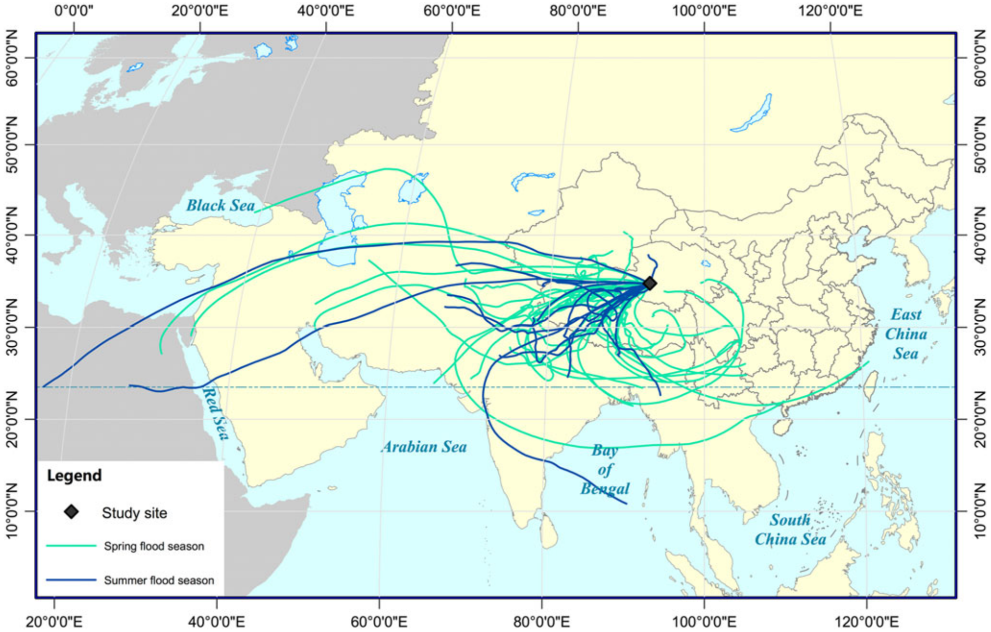

FIGURE 5 Potential moisture sources of precipitation in the study area based on the HYSPLIT model. The black diamond marks the location of the study area. Lines show the starting points of the 10-day backward modeled trajectories

relative to precipitation (Tian et al., 2002). Previous studies have shown that the seasonal dynamics of the soil water content that are altered by freeze–thaw variations in the active layer are the most important controlling factors of hydrological processes in this permafrost watershed (Wang et al., 2009, 2012a). Active seasonal soil water dynamics and seasonal precipitation variations resulted in two peak flows of stream water during the study period (Figures 2 and 8). Extreme fluctuations in precipitation levels may have partially caused variations in the isotopic composition of the stream water. However, the inconsistent isotopic fluctuations of the stream water and precipitation (Figure 4) may indicate that precipitation plays a relatively minor role in the stream water flows, whereas freezing and thawing of the active layer soil plays a central role in controlling river runoff (Wang et al., 2009).

Figure 6 shows the spatiotemporal variations of the isotopic compositions of the stream water. The δD and $\delta^{18}O$ values generally decrease from the smallest to the largest catchments (from 10.9 to 112.5 km^2) with the exception of an increase at 29.3 km^2. In other words, the catchments with areas of 10.9 km^2 (catchment 5) and 29.3 km^2 (catchment 4) have the highest isotopic values. The mean elevations of the five catchments are similar (Table 1); thus, we can disregard "elevation effects" that may affect the isotopic variations (Hren et al., 2009; Cui and Li, 2015). Table 1 shows that the ratio of the area at elevations above 5000 m to the total catchment area is smallest in catchments 5 and 4 (5.7% and 10.5%, respectively). These percentages are 22.2%, 20.2%, and 32.1% for catchments 1 (112.5 km^2), 2 (17.8 km^2), and 3 (54.5 km^2), respectively, which are greater than those of catchments 5 and 4. Thus, catchments 5 and 4 have smaller volumes of snow based on the smaller amounts of snowmelt runoff (Wang et al., 2011). During snowmelt periods, increased isotopic fractionation processes associated with the phase change between solid and liquid water may decrease the meltwater concentrations of heavier deuterium and oxygen isotopes relative to those of snow (Dietermann and Weiler, 2013). Additionally, high solar radiation on the snowpack may cause the kinetic fractionation of water isotopes (Gustafson et al., 2010). Consequently, as the snowmelt runoff in the catchment increases, the δD and $\delta^{18}O$ values decrease. Catchments 5 and 4 have lower snow covers and snowmelt runoff levels and thus higher δD and $\delta^{18}O$ values.

The Pearson's correlation analysis results (Figure 7) show that the soil moisture and soil temperature are closely related to the isotopic compositions of the stream water. The river discharge is negatively correlated with the δD and $\delta^{18}O$ values with Pearson's correlation coefficients (r_p) of −0.41 and −0.38, respectively. The rainfall and air temperatures have smaller effects on the stream water isotope values than the discharge. To identify the major environmental drivers of the stream water isotopic compositions, we conducted a stepwise regression analysis to select the variables that make the greatest contributions and generated multiple linear regression models from the selected variables (Table 3). We used the mean values of the soil moisture and temperature at different depths to fit the multiple linear regression models to prevent multicollinearity of the variables. The multiple regression models for the δD and $\delta^{18}O$ compositions of stream water in the Zuomaokong watershed are described as

$$\delta D = -4.366Ts + 1.2464Ta - 5.4249Q \\ +0.8395Ms - 83.0379 \left(n = 114, R^2 = 0.4268, p<0.001\right), \text{and}$$

$$\delta^{18}O = -0.53Ts + 0.1584Ta - 0.556Q \\ +0.0793Ms - 10.7471 \left(n = 114, R^2 = 0.4395, p<0.001\right),$$

where Ts is the mean soil temperature (°C) at depths of 40, 65, and 120 cm, Ms is the mean soil moisture (%) at depths of 40, 65, and 120 cm, Ta is the air temperature (°C), and Q is the discharge. The results of the multiple linear regression model (Table 3) show that the soil temperature, soil moisture, air temperature, and runoff processes are the main factors that affect the isotopic compositions of the permafrost stream water.

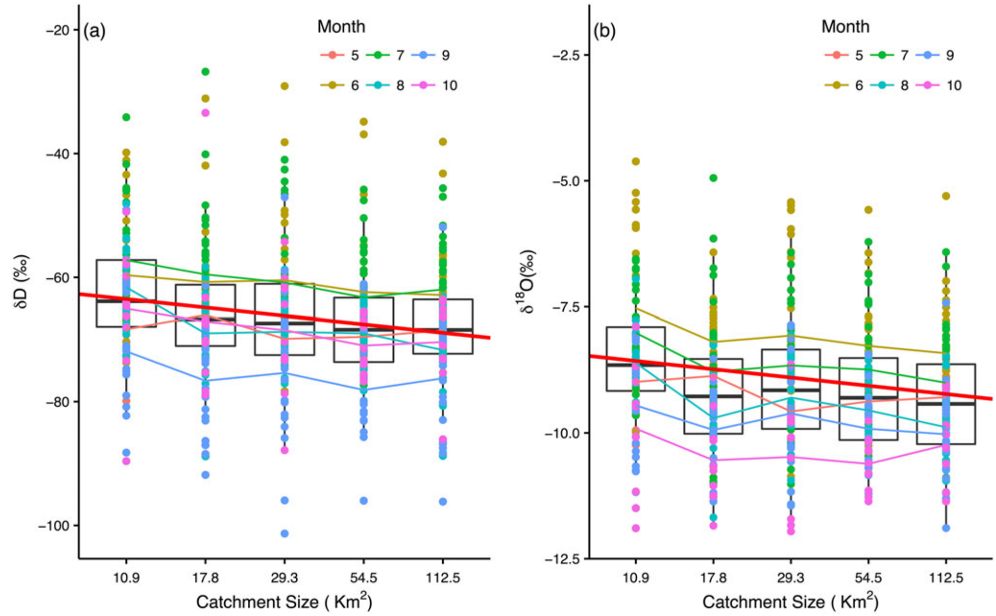

FIGURE 6 Stream water isotopic compositions of the 5 sub-catchments of different spatial scales in the Zuomaokong watershed stratified by month. Box plots show the 25th and 75th percentile quantiles. Colored dots show the sampled isotope data distribution for each group. Mean values of different spatial scales for different months are connected to colored solid lines to show trends between spatial scales. The red line represents the mean trend along catchment size, which was extrapolated over the entire measurement period

As a typical permafrost region, the active soil layer in the Zuomaokong watershed experienced freezing and thawing from May to October, where the active soil layer temperatures were the main factor that controlled runoff variations (Wang et al., 2009, 2011, 2012b). Figure 8 shows the time series of the soil moisture and temperature at different depths during the study period. The temperature of the soil layer started to increase in late June, and the soil moisture levels simultaneously increased rapidly. As a result, the riverine runoff increased (Figure 2) because of increased thawed snow and the limited infiltration below the active layer (Wang et al., 2009). A notable characteristic is that the stream water's isotopic compositions decreased when the active layer started to thaw (Figure 8). Because of the recharge of greater amounts of soil water and groundwater (Tian et al., 2002) after the thawing processes and the more negative isotope values of the deep pore water (Sugimoto et al., 2003; Throckmorton et al., 2016), the decrease of the isotope values was reasonable. We ran nonlinear regressions between the stream water isotopic values and thawed depth; the results are statistically significant ($p < 0.001$ for both δD and δ^{18}O; Figure 9) and show that the deeper the thawed depth, the lower the isotope values. These results are isotopic evidence that thawing of the active soil layer plays an important role in river runoff processes in the permafrost region. The stream water peak in September (Figure 2) produced the lowest isotopic composition of stream water. As the summer flooding season ended and the active soil layer refroze, the isotopic composition of the stream water increased slightly in October.

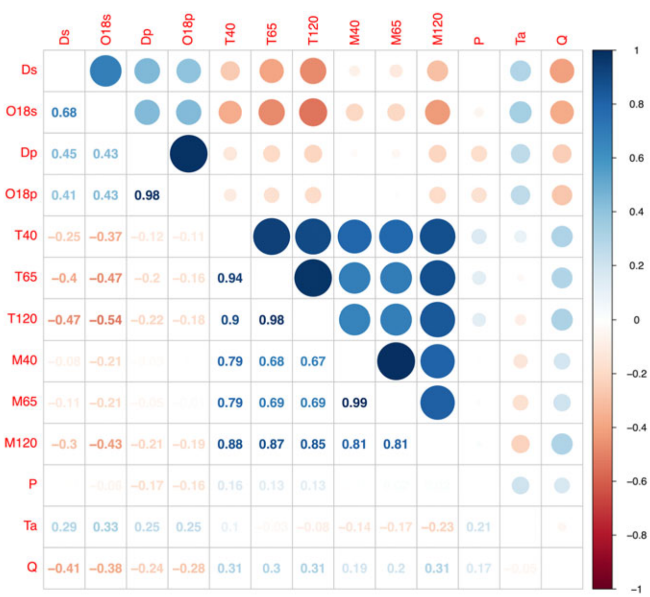

FIGURE 7 Pearson's rank correlation analysis result of stable isotopes and environmental factors. Numbers range from −1 to 1 are Spearman's rank correlation coefficients of variables on horizontal and vertical axes. The larger the number the more significant of the correlation relationship between variables. The size of the circle also shows the significance of the correlation. Abbreviations: Ds, deuterium (‰) in stream water; O18s, oxygen-18 (‰) in stream water; Dp, deuterium (‰) in precipitation; O18p, oxygen-18 (‰) in precipitation; T40, T65, and T120, soil temperature (°C) in 40 cm, 65 cm, and 120 cm depth, respectively; M40, M65, and M120, soil moisture (%) in 40 cm, 65 cm, and 120 cm depth, respectively; P, precipitation (mm); Ta, air temperature (°C); Q, discharge (m3/s)

4.3 | Young water fractions

The daily measured δ^{18}O values of precipitation and stream water were used to estimate the young water fractions (F_{yw}) of the five catchments in the Zuomaokong watershed. Periodic regression analyses were conducted to fit sine wave models to the δ^{18}O time series and calculate the amplitudes of the sinusoidal fits (Figure 10). Each model generated an individual amplitude that was related to the estimated young water

TABLE 3 Multiple linear regression model results of stream water isotopic compositions. Abbreviations: Ts is mean soil temperature (°C) at depths of 40 cm, 65 cm, and 120 cm, Ms is the mean soil moisture (%) at depths of 40 cm, 65 cm, and 120 cm, Ta is the air temperature (°C), and Q is the discharge

Response variable	Component	Estimate	Std. Error	t value	Pr(>|t|)	Multiple R^2	*p*-value
δD	(Intercept)	−83.0379	4.2725	−19.436	<0.001	0.4268	<0.001
	Ts	−4.366	0.7332	−5.955	<0.001		
	Ms	0.8395	0.1803	4.655	<0.001		
	Ta	1.2464	0.248	5.026	<0.001		
	Q	−5.4249	1.4938	−3.632	0.0004		
$\delta^{18}O$	(Intercept)	−10.7471	0.52899	−20.316	<0.001	0.4395	<0.001
	Ts	−0.52999	0.09078	−5.838	<0.001		
	Ms	0.07925	0.02233	3.549	0.0006		
	Ta	0.15842	0.0307	5.16	<0.001		
	Q	−0.55598	0.18496	−3.006	0.003		

fraction (Table 4). The sine regression models of precipitation and stream water were statistically significant ($p < 0.0001$). This method was appropriate because a high sampling frequency will improve the accuracy of the young water fraction calculation (Stockinger et al., 2016). More importantly, this method of quantifying the young water fraction is much more reliable than using the MTT even in heterogeneous and nonstationary catchments (Kirchner, 2016a, b).

Our calculated F_{yw} values for the streamflows of the five catchments in the study area ranged from 9% to 21%. By iteratively solving equations 4 and 6, the threshold ages ranged from 35 to 52 days (Table 4). Catchment 5 has the largest proportion of young water; 21% of the streamflow is less than 35 days old. Catchment 1 has the smallest proportion of young water; 9% of the streamflow is less than 52 days old. An average of 15% of the streamflow in the Zuomaokong watershed is younger than 43 days. The uncertainty ranges of F_{yw} and τ_{yw} are shown in Table 4. Catchment 1 have the largest uncertainty ranges of F_{yw} (0.085–0.113) while catchment 4 have the smallest uncertainty ranges of F_{yw} (0.201–0.210). The uncertainty ranges of

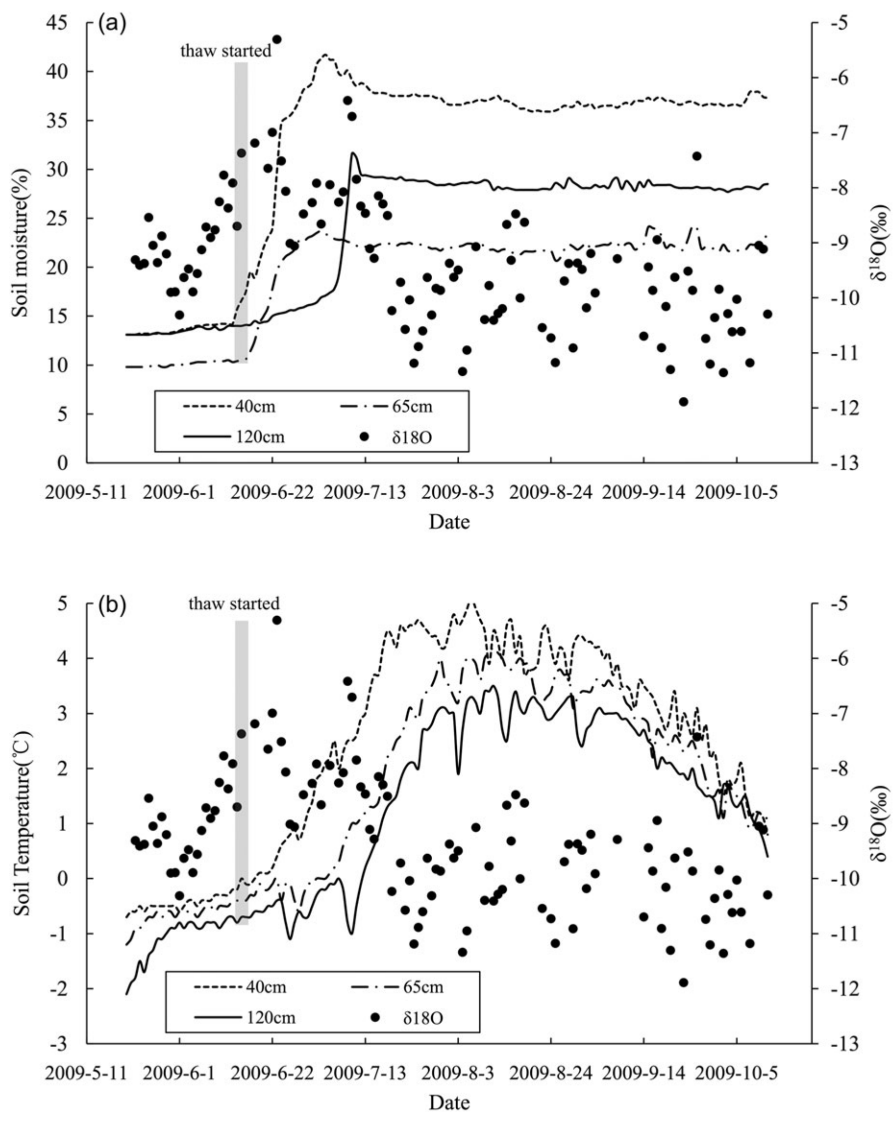

FIGURE 8 The temporal variability of (a) soil moisture and (b) soil temperature in the Zuomaokong watershed for different soil depths during the study period

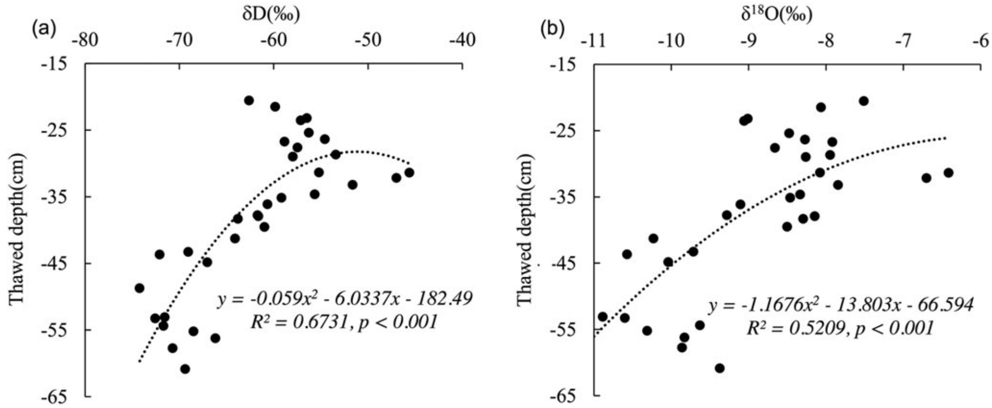

FIGURE 9 Relationships of thawed depth and stable isotopes in stream water

τ_{yw} in catchments 1 and 2 are wider than catchments 4 and 5. These uncertainties indicate that longer length of isotopic data might needed for the estimation of F_{yw}. To our knowledge, these are the first estimates of young streamflow in permafrost catchments on the QTP. These young water fractions correspond well with recent findings of the young water fractions of global catchments (Jasechko

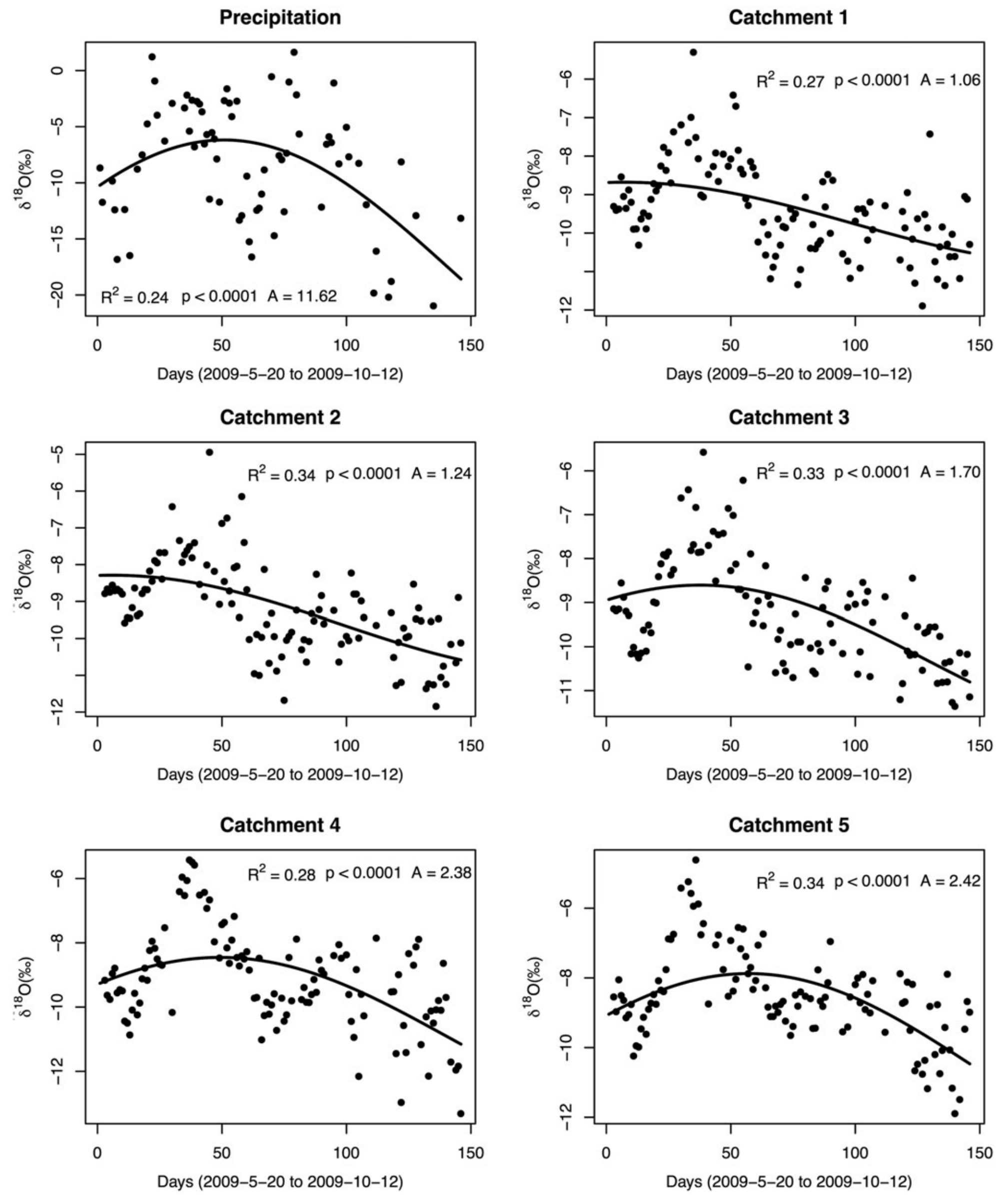

FIGURE 10 Fitted sine regression models of $\delta^{18}O$ for precipitation and stream water in the Zuomaokong watershed. A is the amplitude for each sine regression model

TABLE 4 Stream water estimated amplitude, threshold age for young water and young water fraction in Zuomaokong watershed. α is the shape parameter of the gamma distribution function and F_{yw} is the young water fraction

Catchment	Amplitude	α	τ_{yw} (day)	Uncertainty of τ_{yw} (day)	F_{yw}	Uncertainty of F_{yw}
Precipitation	11.62	—	—		—	—
Catchment 1	1.06	0.4816	52	47–87	0.091	0.085–0.113
Catchment 2	1.24	0.4968	53	48–89	0.107	0.097–0.132
Catchment 3	1.70	0.1462	40	39–41	0.146	0.142–0.155
Catchment 4	2.38	0.0463	36	36–37	0.205	0.201–0.210
Catchment 5	2.42	0.0092	35	35–35	0.208	0.200–0.217
Mean	—	—	43	41–58	0.151	0.145–0.165

et al., 2016). Jasechko et al. (2016) compiled a global precipitation and streamflow isotope database that included 254 rivers and found young water fractions between 4 and 53% for the 10th–90th percentile range with an average F_{yw} of 26%. The mean young water fraction in our study is smaller than this global assessment, which may be due to the permafrost river flow being mainly controlled by thawing and freezing of the active soil layer (Wang et al., 2009). As the temperature increases, the active soil layer recharges the stream network quickly with more old water than in other regions. The substantial proportions of young water imply that even watersheds with long transit times can transmit substantial fractions of soluble contaminants or biogenic substances to aquatic systems over very short time spans (Jasechko et al., 2016). As a region with a fragile ecosystem, these results have important implications for water resource exploitation and protection.

The relationships between F_{yw} and the catchment characteristics were examined using a Pearson's correlation analysis (Table 5). The vegetation coverage of the catchments has a dominant effect on F_{yw}; the percentage of vegetation cover exhibits a strong positive correlation with the young water fraction (r_p = 0.81). F_{yw} is also positively correlated with the percentage of swamp meadow (r_p = 0.43). A previous study in this region found that a decline of vegetation coverage resulted in increases of the temperature and moisture at which the soil starts thawing (Wang et al., 2012b). As a result, the amount of water from the active layer in the streamflow increased. Thus, there would be more "old water" (i.e., older than the young water fraction threshold) and less "young water" (i.e., younger than the young water fraction threshold) and vice versa. Although the vegetation coverage plays an important role in the young water fraction, the substantial unexplained variance suggests that other variables may also be involved. We found that F_{yw} is negatively correlated with the catchment size (r_p = −0.64), mean elevation (r_p = −0.62) and percentage of elevation above 5000 m a.s.l. (r_p = −0.68). The larger catchments represent longer travel times in the stream network, whereas the water in the smaller catchments is younger due to the shorter travel times. F_{yw} is negatively correlated with the mean elevation and percentage of elevation above 5000 m a.s.l., which likely reflects the influence of snowmelt water recharge from higher elevations with long retention times. However, the mean slope gradient of the catchments in our study has little effect on F_{yw} (−0.2). The previous global study found that the young water fraction was inversely correlated with the average catchment slope, which implied that the rivers in plains areas may have more young water than rivers in mountainous areas (Jasechko et al., 2016). The poor relationship between the slope gradient and young water fraction in our study may be due to limited data. Our study shows that the runoff coefficient and young water fraction are poorly related, which is consistent with the global study (Jasechko et al., 2016). Our estimates of the young water fractions based on isotopic tracers contribute to a deeper understanding of hydrological processes and water resource utilization and protection in permafrost regions. As a sensitive permafrost area, the low F_{yw} values indicate that the active soil layer supplies significant water resources. Previous study indicated the vegetation cover was one of the most important factors that control the soil water and thermal cycles in permafrost (Wang, Liu and Li, 2012a) thus should be protected. While the positive correlation between F_{yw} and vegetation implies that higher vegetation cover could potentially increase the speed of chemical contaminants transport along the watershed. Thus, under the premise of vegetation protection, we should pay more attention to prevent the area from being polluted. Further research on the age composition of the streamflow should involve more comprehensive syntheses at multiple scales and consider the basin characteristics to identify the mechanisms of the stream water cycle.

TABLE 5 Pearson correlation coefficients between young water fractions and catchment characteristics

Catchment characteristics	Pearson correlation coefficient
Drainage area	−0.64
Mean slope gradient	−0.2
Mean elevation	−0.62
Area rate of elevation ≥5000 m	−0.68
Mean runoff coefficient	0.22
Swamp meadow	0.43
Vegetation coverage	0.81

5 | CONCLUSIONS

In this study, daily interval precipitation and stream water sampling campaigns were conducted during the 2009 thawing season to identify the characteristics of the stable isotope variations and the young water fractions based on seasonal isotopic cycles. The relationships between the stable isotopes and hydrological permafrost processes in the QTP were explored. We attempted to estimate the proportion of young water with isotope tracers in the QTP permafrost zone for the first time.

The results show that the stable isotope compositions of the precipitation and stream water have significant spatial and temporal variations. The HYSPLIT backwards trajectory model further shows that the moisture sources of the study area are the westerlies, southern monsoons, and East Asian monsoons, which affect the temporal δD and $\delta^{18}O$ variations. The stable isotope variations of the stream water were more constant than those of the precipitation due to the groundwater supplies. The spatial distributions of the stable isotopes in the stream water generally decrease with the spatial scale and are sensitive to snow cover due to isotopic fractionation processes that are associated with the phase change during snowmelt. As a typical permafrost region, the thawing processes of the permafrost's active layer significantly affect the isotope values of the streamflow. The Pearson's rank correlation analysis shows that the soil moisture, soil temperature, air temperature, and discharge are the main controlling factors of the δD and $\delta^{18}O$ variations in the stream water.

We estimated the young water fractions of the studied permafrost catchments using a newly developed approach (Kirchner, 2016a). The results show that the young streamflow in the study area ranged from 9% to 21% and that the young water threshold ages ranged from 35 to 52 days. An average of 15% of the streamflow in the study area is younger than 43 days. The proportions of young water and their relationships with catchment characteristics highlight the need to prevent the water resources in this eco-sensitive zone from being polluted. Further analyses show that the vegetation coverage has significant effects on the young water fraction of the streamflow, whereas the slope gradient and runoff coefficient have minor effects on the young water fractions. Our study of the young water fraction will allow a better understanding of hydrological processes and water resource exploitation and protection in permafrost regions. However, more comprehensive research of permafrost regions is needed in the future. By considering additional potential drivers and observational data at multiple scales, the internal mechanisms of hydrological processes in permafrost regions in the context of climate warming can be assessed more effectively.

ACKNOWLEDGMENTS

This research was supported by the Major Research Plan of the National Natural Science Foundation of China (No. 91547203), the National Basic Research Program of China (973 Program, No. 2013CBA01807), and the National Natural Science Foundation of China (No. 41401044). We would like to thank Fenghuoshan Observation Station of China Railway Northwest Institute for helping our field sampling work.

REFERENCES

Aggarwal, P. K., Romatschke, U., Araguas-Araguas, L., Belachew, D., Longstaffe, F. J., Berg, P., … Funk, A. (2016). Proportions of convective and stratiform precipitation revealed in water isotope ratios. *Nature Geoscience*, *9*(8), 624–629. doi:10.1038/ngeo2739

Craig, H. (1961). Isotopic variations in meteoric waters. *Science*, *133*(3465), 1702–1703. doi:10.1126/science.133.3465.1702

Cui, B.-L., & Li, X.-Y. (2015). Stable isotopes reveal sources of precipitation in the Qinghai Lake Basin of the northeastern Tibetan Plateau. *Science of the Total Environment*, *527-528*, 26–37. doi:10.1016/j.scitotenv.2015.04.105

Cuo, L., Zhang, Y., Zhu, F., & Liang, L. (2014). Characteristics and changes of streamflow on the Tibetan Plateau: A review. *Journal of Hydrology: Regional Studies*, *2*, 49–68. doi:10.1016/j.ejrh.2014.08.004

Dansgaard, W. (1964). Stable isotopes in precipitation. *Tellus*, *16*(4), 436–468. doi:10.1111/j.2153-3490.1964.tb00181.x

Dietermann, N., & Weiler, M. (2013). Spatial distribution of stable water isotopes in alpine snow cover. *Hydrology and Earth System Sciences*, *17*(7), 2657–2668. doi:10.5194/hess-17-2657-2013

Draxler, R. (1998). An overview of the HYSPLIT_4 modelling system for trajectories, dispersion and deposition. *Australian Meteorological Magazine*, *47*(4), 295–308.

Foley J. A., Prentice I. C., Ramankutty N., Levis S., Pollard D., & Sitch S., et al. 1996. An integrated biosphere model of land surface processes, terrestrial carbon balance, and vegetation dynamics. *Global Biogeochemical Cycles*, *10*(4), 603–628. doi:10.1029/96GB02692

Gao, J., Tian, L., Liu, Y., & Gong, T. (2009). Oxygen isotope variation in the water cycle of the Yamzho lake Basin in southern Tibetan Plateau. *Chinese Science Bulletin*, *54*(16), 2758–2765. doi:10.1007/s11434-009-0487-6

Gat, J. R. (1996). Oxygen and hydrogen isotopes in the hydrologic cycle. *Annual Review of Earth and Planetary Sciences*, *24*(1), 225–262.

Gustafson, J. R., Brooks, P. D., Molotch, N. P., & Veatch, W. C. (2010). Estimating snow sublimation using natural chemical and isotopic tracers across a gradient of solar radiation. *Water Resources Research*, *46*(12), W12511. doi:10.1029/2009WR009060

Hinton, M. J., Schiff, S. L., & English, M. C. (1994). Examining the contributions of glacial till water to storm runoff using two- and three-component hydrograph separations. *Water Resources Research*, *30*(4), 983–993. doi:10.1029/93WR03246

Hiyama, T., Asai, K., Kolesnikov, A. B., Gagarin, L. A., & Shepelev, V. V. (2013). Estimation of the residence time of permafrost groundwater in the middle of the Lena River basin, eastern Siberia. *Environmental Research Letters*, *8*(3), 035040. doi:10.1088/1748-9326/8/3/035040

Hren, M. T., Bookhagen, B., Blisniuk, P. M., Booth, A. L., & Chamberlain, C. P. (2009). $\delta^{18}O$ and δD of streamwaters across the Himalaya and Tibetan Plateau: Implications for moisture sources and paleoelevation reconstructions. *Earth and Planetary Science Letters*, *288*(1–2), 20–32. doi:10.1016/j.epsl.2009.08.041

Jasechko, S., Kirchner, J. W., Welker, J. M., & McDonnell, J. J. (2016). Substantial proportion of global streamflow less than three months old. *Nature Geoscience*, *9*(2), 126–129. doi:10.1038/ngeo2636

Kirchner, J. W. (2016a). Aggregation in environmental systems-Part 1: Seasonal tracer cycles quantify young water fractions, but not mean transit times, in spatially heterogeneous catchments. *Hydrology and Earth System Sciences*, *20*(1), 279–297. doi:10.5194/hess-20-279-2016

Kirchner, J. W. (2016b). Aggregation in environmental systems-Part 2: Catchment mean transit times and young water fractions under hydrologic nonstationarity. *Hydrology and Earth System Sciences*, *20*(1), 299–328. doi:10.5194/hess-20-299-2016

Klaus, J., & McDonnell, J. J. (2013). Hydrograph separation using stable isotopes: Review and evaluation. *Journal of Hydrology*, *505*, 47–64.

Li, S.-L., Yue, F.-J., Liu, C.-Q., Ding, H., Zhao, Z.-Q., & Li, X. (2014). The O and H isotope characteristics of water from major rivers in China. *Chinese Journal of Geochemistry*, *34*(1), 28–37. doi:10.1007/s11631-014-0015-5

Maher, K. (2010). The dependence of chemical weathering rates on fluid residence time. *Earth and Planetary Science Letters*, *294*(1–2), 101–110. doi:10.1016/j.epsl.2010.03.010

McDonnell J. J., McGuire K., Aggarwal P., Beven K. J., Biondi D., … Destouni G. 2010. How old is streamwater? Open questions in catchment transit time conceptualization, modelling and analysis (KJ Beven, ed.). *Hydrological Processes 24* (12): 1745–1754 DOI: 10.1002/hyp.7796

McGuire, K. J., & McDonnell, J. J. (2006). A review and evaluation of catchment transit time modeling. *Journal of Hydrology*, *330*(3–4), 543–563. doi:10.1016/j.jhydrol.2006.04.020

Pearce, A. J., Stewart, M. K., & Sklash, M. G. (1986). Storm runoff generation in humid headwater Catchments: 1. Where Does the Water

Come From? *Water Resources Research*, *22*(8), 1263–1272. doi:10.1029/WR022i008p01263

R Core Team (2016). *R: A language and environment for statistical computing*. Vienna, Austria: Available at: https://www.R-project.orgR Foundation for Statistical Computing.

Rodgers, P., Soulsby, C., & Waldron, S. (2005). Stable isotope tracers as diagnostic tools in upscaling flow path understanding and residence time estimates in a mountainous mesoscale catchment. *Hydrological Processes*, *19*(11), 2291–2307. doi:10.1002/hyp.5677

Rozanski, K., Araguas-Araguas, L., & Gonfiantini, R. (1992). Relation between long-term trends of oxygen-18 isotope composition of precipitation and climate. *Science*, *258*(5084), 981–985. doi:10.1126/science.258.5084.981

Sánchez-Murillo, R., Birkel, C., Welsh, K., Esquivel-Hernández, G., Corrales-Salazar, J., … Boll, J. (2016). Key drivers controlling stable isotope variations in daily precipitation of Costa Rica: Caribbean Sea versus Eastern Pacific Ocean moisture sources. *Quaternary Science Reviews*, *131*, 250–261. doi:10.1016/j.quascirev.2015.08.028

Sánchez-Murillo, R., Brooks, E. S., Elliot, W. J., & Boll, J. (2015). Isotope hydrology and baseflow geochemistry in natural and human-altered watersheds in the Inland Pacific Northwest, USA. *Isotopes in Environmental and Health Studies*, *51*(2), 231–254. doi:10.1080/10256016.2015.1008468

Siegenthaler, U., & Oeschger, H. (1980). Correlation of 18O in precipitation with temperature and altitude. *Nature*, *285*(5763), 314–317. doi:10.1038/285314a0

Soulsby, C., Tetzlaff, D., Rodgers, P., Dunn, S., & Waldron, S. (2006). Runoff processes, stream water residence times and controlling landscape characteristics in a mesoscale catchment: An initial evaluation. *Journal of Hydrology*, *325*(1–4), 197–221. doi:10.1016/j.jhydrol.2005.10.024

Stein, A. F., Draxler, R. R., Rolph, G. D., Stunder, B. J. B., Cohen, M. D., & Ngan, F. (2015). NOAA's HYSPLIT atmospheric transport and dispersion modeling system. *Bulletin of the American Meteorological Society*, *96*(12), 2059–2077. doi:10.1175/BAMS-D-14-00110.1

Stockinger, M. P., Bogena, H. R., Lücke, A., Diekkrüger, B., Cornelissen, T., & Vereecken, H. (2016). Tracer sampling frequency influences estimates of young water fraction and streamwater transit time distribution. *Journal of Hydrology*. doi:10.1016/j.jhydrol.2016.08.007

Streletskiy, D. A., Tananaev, N. I., Opel, T., Shiklomanov, N. I., Nyland, K. E., Streletskaya, I. D., … Shiklomanov, A. I. (2015). Permafrost hydrology in changing climatic conditions: Seasonal variability of stable isotope composition in rivers in discontinuous permafrost. *Environmental Research Letters*, *10*(9), 095003. doi:10.1088/1748-9326/10/9/095003

Sugimoto, A., Naito, D., Yanagisawa, N., Ichiyanagi, K., Kurita, N., Kubota, J., … Fedorov, A. N. (2003). Characteristics of soil moisture in permafrost observed in East Siberian taiga with stable isotopes of water. *Hydrological Processes*, *17*(6), 1073–1092. doi:10.1002/hyp.1180

Tekleab, S., Wenninger, J., & Uhlenbrook, S. (2014). Characterisation of stable isotopes to identify residence times and runoff components in two meso-scale catchments in the Abay/Upper Blue Nile basin, Ethiopia. *Hydrology and Earth System Sciences*, *18*(6), 2415–2431. doi:10.5194/hess-18-2415-2014

Throckmorton, H. M., Newman, B. D., Heikoop, J. M., Perkins, G. B., Feng, X., … Graham, D. E. (2016). Active layer hydrology in an Arctic tundra ecosystem: Quantifying water sources and cycling using water stable isotopes. *Hydrological Processes*. doi:10.1002/hyp.10883

Tian, L., Masson-Delmotte, V., Stievenard, M., Yao, T., & Jouzel, J. (2001). Tibetan Plateau summer monsoon northward extent revealed by measurements of water stable isotopes. *Journal of Geophysical Research: Oceans (1978–2012)*, *106*(D22), 28081–28088. doi:10.1029/2001JD900186

Tian, L., Yao, T., Shen, Y., Yang, M., Ye, B., Numaguti, A., & Tsujimura, M. (2002). Study on stable isotope in river water and precipitation in Naqu River basin. *Adcances in Water Science*, *12*(2), 206–210.

Wang, B., & French, H. M. (1995). Permafrost on the Tibet Plateau, China. *Quaternary Science Reviews*, *14*(3), 255–274. doi:10.1016/0277-3791(95)00006-B

Wang, G., Hu, H., & Li, T. (2009). The influence of freeze–thaw cycles of active soil layer on surface runoff in a permafrost watershed. *Journal of Hydrology*, *375*(3), 438–449. doi:10.1016/j.jhydrol.2009.06.046

Wang, G., Liu, G., & Li, C. (2012a). Effects of changes in alpine grassland vegetation cover on hillslope hydrological processes in a permafrost watershed. *Journal of Hydrology*, *444-445*(C), 22–33. doi:10.1016/j.jhydrol.2012.03.033

Wang, G., Liu, G., & Liu, L. (2011). Spatial scale effect on seasonal streamflows in permafrost catchments on the Qinghai-Tibet Plateau. *Hydrological Processes*, *26*(7), 973–984. doi:10.1002/hyp.8187

Wang, G., Mao, T., Chang, J., & Liu, G. (2015). Soil temperature-threshold based runoff generation processes in a permafrost catchment. *The Cryosphere Discussions*, *9*(6), 5957–5978. doi:10.5194/tcd-9-5957-2015

Wang, G. X., Li, Y. S., Hu, H. C., & Wang, Y. (2008). Synergistic effect of vegetation and air temperature changes on soil water content in alpine frost meadow soil in the permafrost region of Qinghai-Tibet. *Hydrological Processes*, *22*(17), 3310–3320. doi:10.1002/hyp.6913

Wang, G. X., Liu, G. S., Li, C. J., & Yang, Y. (2012b). The variability of soil thermal and hydrological dynamics with vegetation cover in a permafrost region. *Agricultural and Forest Meteorology*, *162*, 44–57. doi:10.1016/j.agrformet.2012.04.006

Winnick, M. J., Chamberlain, C. P., Caves, J. K., & Welker, J. M. (2014). Quantifying the isotopic 'continental effect'. *Earth and Planetary Science Letters*, *406*, 123–133. doi:10.1016/j.epsl.2014.09.005

Yao, T., Masson Delmotte, V., Gao, J., Yu, W., Yang, X., … Risi, C. (2013). A review of climatic controls on δ18O in precipitation over the Tibetan Plateau: Observations and simulations. *Reviews of Geophysics*, *51*(4), 525–548. doi:10.1002/rog.20023

Yao, T., Zhou, H., & Yang, X. (2009). Indian monsoon influences altitude effect of δ18O in precipitation/river water on the Tibetan Plateau. *Scientific Bulletin*, *54*(16), 2724–2731. doi:10.1007/s11434-009-0497-4

Yu, W., Yao, T., Tian, L., Ma, Y., Kurita, N., Ichiyanagi, K., … Sun, W. (2007). Stable isotope variations in precipitation and moisture trajectories on the western Tibetan Plateau, China. *Arctic Antarctic and Alpine Research*, *39*(4), 688–693.

Zhang, Y., Ohata, T., & Kadota, T. (2003). Land-surface hydrological processes in the permafrost region of the eastern Tibetan Plateau. *Journal of Hydrology*, *283*(1–4), 41–56. doi:10.1016/S0022-1694(03)00240-3

Zhao, L., Yin, L., Xiao, H., Cheng, G., Zhou, M., Yang, Y., … Zhou, J. (2011). Isotopic evidence for the moisture origin and composition of surface runoff in the headwaters of the Heihe River basin. *Chinese Science Bulletin*, *56*(4–5), 406–415. doi:10.1007/s11434-010-4278-x

SUPPORTING INFORMATION

Additional Supporting Information may be found online in the supporting information tab for this article.

How to cite this article: Song C. Wang G. Liu G. Mao T. Sun X. Chen X. Stable isotope variations of precipitation and streamflow reveal the young water fraction of a permafrost watershed, *Hydrological Processes*. 2016. doi: 10.1002/hyp.11077